CrVI and Trace Element Contaminated Groundwater Systems Connected with Ophiolitic Rocks

Z. Hatipoglu-Bagci[1] · C. S. Bayari[2]

Abstract

The level and distribution of chromium (as total chromium and CrVI) and other trace elements were investigated from surface and groundwater samples collected over three periods (n = 155) from Mersin (Turkey) in terms of their origins and potential health risk. The maximum total chromium is 41 µg/L and some of the samples have CrVI contents above 5 µg/L, which is the maximum permissible level of CrVI under Italian regulations. The dominant water facies are Ca–HCO$_3$ and Mg–HCO$_3$ types based on the Piper diagram. The Ca–HCO$_3$ type waters originate mainly from interaction with carbonate rocks, and the Mg–HCO$_3$ type waters originate from serpentinite dissolution. Chromium contents are higher in Mg–HCO$_3$ water types and the highest concentrations are found in samples from ophiolitic rocks and industrial areas. The As, Fe, Pb, Al, and Ni contents of some samples are above the EU limits in industrial areas.

Keywords Contamination · Chromium · CrVI · Groundwater · Surface water · Mersin

Groundwater quality degradation is a common problem in Mediterranean countries. A common approach for tackling water resource management problems is of urgent importance, especially with regards to CrVI contamination. To address this problem, the EU-ERANETMED CrITERIA project was designed to assist water resource management organizations with an optimization tool with the involvement of partner countries (Greece, Italy, Turkey, Cyprus, Jordan, Oman).

Chromium is a toxic element and can be found in different oxidation states, of which CrIII and CrVI predominate in the environment. CrVI is more stable and toxic and has higher solubility and mobility in natural water than CrIII (Silva et al. 2008). Human activity was previously considered to be the only source of CrVI in groundwater, however, recent studies have shown that high CrVI contents may result from natural processes including CrIII oxidation in ultramafic rocks, particularly serpentinites in ophiolite complexes under favorable pH and redox conditions (Oze et al. 2004, 2007; Dermatas et al. 2015).

The International Agency for Research on Cancer classified CrVI compounds as carcinogenic (Group 1) on the basis of evidence provided from occupational studies (EFSA CONTAM Panel 2014). According to EU legislation, the maximum Cr limit in drinking water is 50 µg/L (EU 98/83/EC). However, this limit will likely undergo reevaluation in the near future owing to health concerns regarding CrVI toxicity. For example, Italy established a maximum permissible CrVI level in drinking water of 5 µg/L. CrVI and CrIII can convert back and forth in water, as well as in the human body, depending on environmental conditions. The Environmental Protection Agency (EPA) regulation therefore assumes that Cr is 100% CrVI, the more toxic form, to address the greatest potential risk (EPA 2019). Because CrIII solubility in natural water with typical pH (6.5–8.5) is significantly lower than 5 µg/L, naturally occurring chromium should be attributed mainly to CrVI (Mitrakas et al. 2012).

Recent studies have shown that CrVI can reach high levels in groundwater that interacts with ophiolitic rocks. Since Mersin is located in the discharge domain of a large drainage area consisting of extensive outcrops of ophiolitic rocks, it

✉ Z. Hatipoglu-Bagci
  zubeyde@mersin.edu.tr

1   Department of Geological Engineering, Mersin University, Ciftlikkoy, 33343 Mersin, Turkey

2   Hydrogeological Engineering Section, Department of Geological Engineering, Hacettepe University, 06532 Ankara, Turkey
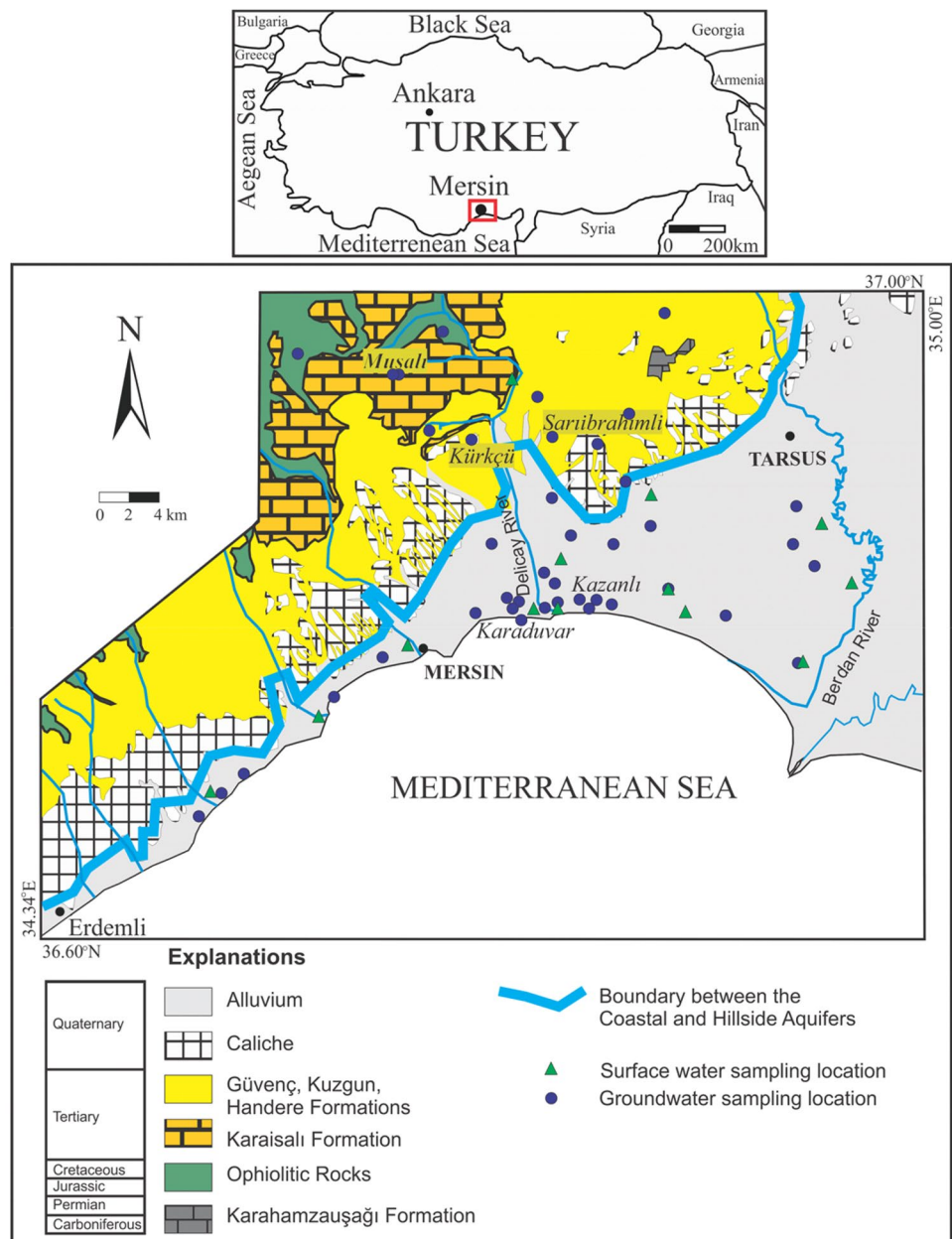
was selected as the study area. The aim of this study is to investigate the level, distribution and source of chromium in surface and groundwater in the study area where geogenic and anthropogenic chromium contamination sources are possible, and to examine the water quality with other contaminants related to health risks.

The study area covers the cities of Mersin and Tarsus and their vicinity along the southern coast of Turkey (Fig. 1). The area covers ~800 km^2 and is situated between 34° 20′ and 34° 57′ N and 36° 38′ and 37° 00′ E. The Mediterranean climate is warm with draught summers and moderately cool, mild, and rainy winters. There are eight perennial rivers, which originate from karst springs in the mountainous

section, that have a total drainage area of 4062 km^2. The Berdan River is the largest stream in the area with a mean annual discharge of 39.73 m^3/s, whereas the mean annual discharges of the other rivers are less than 5 m^3/s (Hatipoglu 2004).

This region consists of a mixture of settled, agricultural, and industrial areas (Supplementary material Fig. S1). The main industrial areas are concentrated around the districts of Kazanlı-Karaduvar and Sarıibrahimli-Kürkçü. The oldest industries in the Kazanlı-Karaduvar area include a fertilizer factory, soda factory, chrome factory, and an oil refinery. Oil storage facilities have become widespread in this region in recent decades and a range of environmental problems

Fig. 1 Location, geology, and sampling map of the study area (modified after Senol et al. 1998; Hatipoglu et al. 2009)

have arisen because of these facilities' associated pipelines (DSI 2016). The Mersin municipality wastewater treatment plant is also located in this region, and the Mersin free zone and port are located in the west. Large-scale glass factories, a cement factory, and two organized industrial zones are located around Sarıibrahimli-Kürkçü in the shallow hillside areas. Settlement areas are located in Mersin and Tarsus city centers and villages. The remaining areas are used as agricultural lands with widespread irrigation and drainage canal systems. The 2014 population of Mersin central districts and Tarsus was ~ 1,300,000 (DSI 2016).

Most of the study area is located on a low-lying coastal plain and hillside area of the Taurus Mountains. The age of the stratigraphic sequence ranges from Carboniferous to Quaternary. The Carboniferous age Karahamzauşağı Formation contains limestone, schist, and quartz units, and is tectonically overlain by an ophiolitic mélange that includes Mesozoic limestone blocks (Senol et al. 1998). From top to bottom, the Mersin ophiolite consists of chromitite-bearing and strongly serpentinized mantle peridotites, ultramafic cumulates (dunite, wehrlite, pyroxenite), mafic layered cumulates (leucogabbro, olivine-gabbro, anorthosite) and alkaline to tholeiitic basaltic volcanic rocks in association with deep marine sediments (Parlak 1996). This geologic sequence outcrops in the northern mountainous section of the study area. The units are covered by Neogene-aged Gildirli, Karaisalı, Güvenç, Kuzgun, and Handere formations. The Karaisalı formation consists mainly of limestone, and the other formations are composed of marl, limestone, sandstone, siltstone, claystone, and gypsum alternations (Senol et al. 1998). These formations are covered by caliche, a secondary calcium carbonate deposit, along the boundary with Quaternary alluvium that forms the coastal plain (Fig. 1).

The region consists of two main hydrogeological areas: a coastal aquifer and a hillside aquifer. The low-yield hillside aquifer is formed of mainly cemented Neogene formations as well as ophiolitic rocks. The high-yield coastal aquifer is formed of uncemented granular Quaternary units that represent a deltaic environment. A Paleozoic karst aquifer extends beneath the hillside aquifer toward the Mediterranean Sea and covers most of the area in the Taurus Mountains in the north (Hatipoglu et al. 2009).

Hatipoglu et al. (2009) characterized the groundwater system of the same area using hydrochemical and isotopic data and a groundwater flow model. The results showed three different types of hydrochemical facies: (1) a fresh groundwater zone of Ca/Mg–HCO_3 facies; (2) seawater intrusion; and (3) previously saline groundwater flushed by Ca/Mg–HCO_3 type water. Ca–HCO_3 facies suggests a groundwater composition that is typical of carbonate aquifers, and the dominance of Mg^{2+} in some samples is attributed to groundwater contact with ophiolitic rocks. This study also showed that most of the groundwater along the coastal zone is supplied by the Taurus mountain belt, which includes extensive ophiolitic outcropping. Other studies have investigated smaller parts of the study area. For example, Guler et al. (2012) assessed the hydrochemistry of the Tarsus coastal plain using various techniques and indicated hydrochemical variability factors such as water rock interaction, salinization by seawater intrusion, evaporite dissolution, and geogenic/anthropogenic Cr, Fe, and Mn. Guler et al. (2013) studied heavy metal concentrations including Cr in groundwater samples from the Karaduvar coastal aquifer and a petroleum hydrocarbon-contaminated site, and reported that samples contained Cr contents higher than 20 µg/L.

Materials and Methods

A total of 155 samples, ~ 10 surface water and 40 groundwater samples for each campaign representing dry and rainy seasons, were collected and analyzed to characterize the water quality in May 2017, October–November 2017, and May–June 2018 (Fig. 1, Supplementary material Tables S1–S3). The water-sampling protocol prepared in the CrITERIA project based on standard analytical procedures (e.g. APHA 2005) was used for sample collection, preservation, and analysis. The temperature, pH, specific electrical conductivity (EC), dissolved oxygen (DO), and redox potential (ORP) were measured using a YSI ProPlus multiparameter instrument. EC and pH measurements were calibrated against traceable standard solutions in the laboratory and the DO calibration was carried out in-situ against atmospheric pressure. Samples were filtered by 0.45-µm membrane filters using disposable syringes and acidified with HNO_3 for analysis of major cations and trace metal analyses in the field. Ion chromatography, ICP-MS, and titration methods were used for major and trace element analyses. The spectrophotometric diphenylcarbazide method was used to determine CrVI. Three sessions of major ion analyses were conducted at the Water Chemistry Laboratory of Hacettepe University. Trace elements of the first and second session samples were measured in the same laboratory and the third session was conducted at the Central Laboratory of Middle East Technical University. The ionic balance errors are less than ± 5% for all samples and the total cation or anion concentrations are in agreement with the field EC measurements. Three randomly selected samples were analyzed at Eurofin Laboratory (USA) to check the accuracy of the chemical analyses and two of the laboratory analyses are compatible. As mentioned previously, the total Cr under natural conditions is mainly attributed to CrVI (Mitrakas et al. 2012), and the correlation coefficient (r) between total Cr and CrVI contents of the collected water samples is 0.86. The difference of these two variables might be attributed to different analytical methods.

Results and Discussion

The groundwater temperatures ranged between 13.3 and 24.5°C during the three periods and decreased with increasing elevation, except in the southern part of Tarsus. The pH ranged from 6.74 to 8.40 and most samples were off slightly alkaline character. There are no significant differences between the dry and rainy season temperatures and pH of the groundwater samples. The EC ranges from 272 to 7508 μS/cm with higher values obtained from samples in the Sarıbahimli-Kürkçü area and coastal zone. The ORP of the groundwater samples ranged between − 119.1 and 625 mV and most are of an oxidizing character.

The major cation and anion concentrations of the groundwater samples are plotted on Piper diagrams (Supplementary material Fig. S2), which indicate that the most common hydrochemical facies of the wet and dry seasons are Ca–HCO$_3$ and Mg–HCO$_3$. A few groundwater samples include Na–Cl, Na–HCO$_3$, Ca–Cl, Mg–Cl, Mg–SO$_4$, and Na–SO$_4$. The surface waters are represented by Ca–HCO$_3$, Mg–HCO$_3$, Na–Cl, and Na–HCO$_3$ facies (Supplementary material Fig. S3).

When a water sample plots close to the Ca–Mg edge along a line on a Piper diagram, this indicates a variation from Ca-rich to Mg-rich facies produced by the interaction of different lithologies or mixing of Ca–HCO$_3$ and Mg–HCO$_3$ (Bruni et al. 2002; Margiotta et al. 2012). On the Ca vs. Mg binary plot, Mg-HCO$_3$ type waters from serpentinites fall below the 1:3 line of Ca/Mg. In contrast, Ca-HCO$_3$ type waters plot above the 1:1 line. Samples that plot between the 1:1 and 1:3 lines indicate mixing of the Ca-HCO$_3$ and serpentine derived Mg-HCO$_3$ type waters (Margiotta et al. 2012). In the present study, two water groups are observed on the Ca vs. Mg binary plot. Ca–HCO$_3$ waters plot above the 1:1 line and mixtures of Ca–HCO$_3$ and serpentine-derived Mg–HCO3 type waters plot between the 1:1 and 1:3 lines (Fig. 2a).

A Mg–SiO$_2$–HCO$_3$ ternary diagram is also useful for distinguishing Mg–HCO$_3$ and Ca–HCO$_3$ facies and to investigate water–rock interaction processes that affect Mg–HCO$_3$ waters. The diagram also shows expected compositions of aqueous phases produced by Mg-bearing rocks. The stoichiometry of the different mineral phases is reflected by variable SiO$_2$/Mg and SiO$_2$/HCO$_3$ ratios on this plot. The HCO$_3$/Mg molar ratio is significantly > 2 in the Ca–HCO$_3$ type waters because of the balance between dissolved HCO$_3$ and Ca ions. In addition, samples that point toward the HCO$_3$ apex suggest that in most cases, HCO$_3$ is driven mainly by carbonate dissolution. HCO$_3$/Mg molar ratios that are close to 2 in Mg–HCO$_3$ waters and plot slightly to the left of the serpentine point indicate that Mg–HCO$_3$ type waters are produced through incongruent serpentine dissolution (Fantoni et al. 2002; Margiotta et al. 2012). For the study area, similar to Ca vs. Mg binary plot, Ca–HCO$_3$ type water produced from carbonate rock dissolution and Mg–HCO$_3$ water are derived from interaction with serpentine (Fig. 2b).

Na–Cl, Na–HCO$_3$, and Ca–Cl facies are observed on the Piper diagram (Supplementary material Figs. S2, S3) and appear to be related to salinization. When seawater increases, Cl concentrations increase. Na will initially increase and result as Na–Cl facies, but when cation exchange occurs, Na will be partially replaced by Ca and Ca–Cl facies occur, which is a direct indicator of salinization
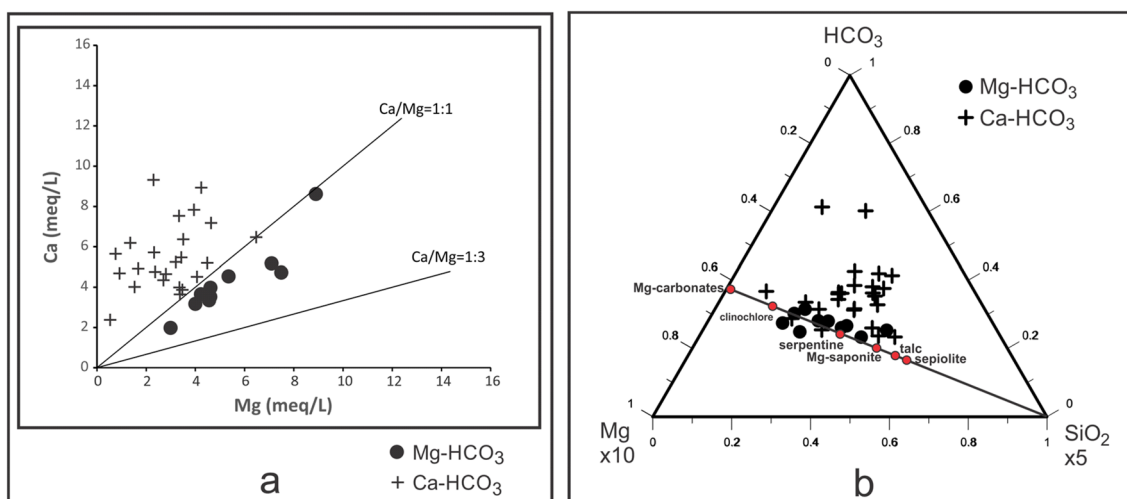

Fig. 2 a Bivariate plot of Ca vs. Mg for May–June 2018 groundwater samples. **b** Ternary diagram of Mg–SiO$_2$–HCO$_3$ for May–June 2018 samples groundwater samples. Red circles represent the expected aqueous phase compositions produced by CO$_2$-driven dissolution of Mg-bearing solid phases (Fantoni et al. 2002; Margiotta et al. 2012)

(Camp and Walraevens 2008). Freshwater intrusion (flushing) leads to Ca and Mg adsorption by the ion exchangers upon Na release. This process can increase the formation of Na–HCO$_3$ type water (Amiri et al. 2016). Increasing Na, Cl, Ca, and SO$_4$ concentrations indicate evaporite dissolution (Camp and Walraevens 2008) from Tertiary formations for inland areas of the study area.

The results show that none of the surface and groundwater samples have total Cr contents above the 50 μg/L maximum limit of the EU drinking water standard, but some samples have CrVI contents above 5 μg/L, which is maximum permissible level of CrVI according to the Italian regulation. Because the EPA's regulation assumes that total Cr represents 100% CrVI (EPA 2019), total chromium contents are presented. In the first and third periods, which represent the rainy season, the highest total Cr contents are 27 and 31 ppb, respectively, in groundwater samples collected around the ophiolite rocks in Musalı, which is located at high elevations and far from the industrial areas (Supplementary material Fig. S4). In the first period, groundwater samples with total Cr content in excess of 5 μg/L were collected from Kazanlı and south of the Sarıibrahimli industrial areas. In the second period, which represents the dry season, the highest total Cr content was 41 μg/L in the Kazanlı region located on the coast where industrial facilities are widespread. For the second dry period, most of the total Cr contents are higher than the first rainy period and the mean total Cr contents increase from 2.0 to 5.6 μg/L. Groundwater samples collected from Musalı, Sarıibrahimli, and Kazanlı, and some samples from Karaduvar and the western part of Mersin in the settlement areas show total Cr contents in excess of 5 μg/L during this period. In the third period, representing the rainy season, samples with total Cr content in excess of 5 μg/L show a similar spatial distribution to the second season with a mean of 5.3 μg/L. Samples collected from a drainage canal located in the southeast part of Sarıibrahimli and some samples from drainage canals connected to the industrial areas in the south and southwest part of Tarsus show total Cr contents higher than 5 μg/L.

The distribution of Cr in groundwaters in the study area is congruent with water chemistry. For the October–November 2017 sampling period, three samples of Ca–HCO$_3$ type waters, which represent 20% of this group, show total Cr concentrations above 5 ppb with a maximum of 7.9 μg/L. Nine samples of Mg-HCO$_3$ type waters, which represent 75% of this group, show Cr concentrations above 5 ppb with a maximum of 41.3 ppb. For Ca–HCO$_3$ and Mg–HCO$_3$ type waters, the different Cr distribution possibly indicates different Cr contents of the rocks (Fantoni et al. 2002).

The most common heavy metals in the surface and groundwater samples are As, Fe, Pb, Al, and Ni, which are found to be above the EU limits (10, 200, 10, 200, and 20 μg/L, respectively) in some of the samples and therefore pose a severe health threat. As contents vary between < 0.001 and 76.3 μg/L in the three periods of the surface and groundwater samples. Fe contents range from < 0.001 to 844 μg/L, Pb contents vary between < 0.001 and 81 μg/L, Al contents vary between < 0.001 and 4286 μg/L, and Ni contents range from < 0.001 to 32.9 μg/L for the surface and groundwater samples. Heavy metal contents above EU limits are mainly observed in the Sarıibrahimli-Kürkçü and Kazanlı-Karaduvar groundwater samples and others were mainly collected from drainage canals connected to the industrial areas in south-southwest Tarsus (Supplementary material Figs. S5, S6).

Panagiotakis et al. (2015) showed that the presence of Cr-rich geologic formations, absence of co-contaminants, and presence of Ni contents (without clear spatial or linear correlation with CrVI) are indicative of geogenic origins of Cr. For dry period groundwater samples without heavy metal contamination and low heavy metal contents, the correlation coefficients between Cr and other heavy metals (As, Fe, Pb, Al, Ni) are less than 0.27. It is therefore concluded that chromium is of geogenic origin for these samples. On the other hand, groundwater samples with heavy metal contamination above EU limits collected from Sarıibrahimli-Kürkçü and Kazanlı-Karaduvar show significantly high linear correlations and correlation coefficients between Cr and other heavy metals (As, Pb, Al, Ni) are greater than 0.93. This indicates that these samples also have anthropogenic Cr contamination because of the increased industrial density in these areas. Also t-test indicates that statistically significant differences between the means of Fe, As and Al contents of two groups of groundwater samples, which are with and without heavy metal contamination, at the 95% confidence level.

Most of the groundwater samples have NO$_3$ contents that are close to or above the limit of 50 mg/L determined by the EU drinking water standard for NO$_3$, which may result from intense long-standing fertilizer application. High nitrate concentrations have been shown to increase CrVI mobility (Dermatas et al. 2015). In the first and third periods, the maximum NO$_3$ contents of groundwater samples in the Kürkçü samples are 134 and 182 mg/L, respectively. In the second period, the maximum NO$_3$ content is 134 mg/L in the western coastal part of Mersin. The mean NO$_3$ contents of the first, second, and third periods are 36, 40, and 47 mg/L, respectively. The nitrate contents are lower in surface waters than in groundwater samples, and the mean NO$_3$ contents in all three periods are 6, 7, and 7 mg/L, respectively.

The present study was aim to investigate the level, distribution and source of Cr and other contaminants in surface and groundwater in Mersin. The conclusions obtained from this study are as follows: (1) According to the geological structure of the study area, the Ca–HCO$_3$ waters are derived from rocks containing Ca-bearing minerals mainly carbonate

rocks, and the Mg–HCO$_3$ type waters originate from serpentinite dissolution, (2) none of the surface and groundwater samples have total Cr contents above the 50-µg/L maximum limit of the EU drinking water standard, but some samples have CrVI contents above 5 µg/L, which is maximum permissible level of CrVI according to the Italian regulation, (3) some of the surface and groundwater samples As, Fe, Pb, Al, and Ni contents are found to be above the EU limits, (4) Mg–HCO$_3$ type waters having higher Cr contents than Ca–HCO$_3$ type of waters possibly indicates different Cr contents of the rocks, (5) presence of Ni and the absence of co-contaminants are possibly indications of geogenic Cr origins for sites without heavy metal contamination, (6) presence of other contaminants with Cr and high linear correlation coefficients between Cr and As, Pb, Al, and Ni indicate anthropogenic components of the contamination in Kazanlı-Karaduvar and Sarıbrahimli-Kürkçü industrial regions.

References

Amiri V, Nakhaei M, Lak R, Kholghi M (2016) Investigating the salinization and freshening processes of coastal groundwater resources in Urmia aquifer NW Iran. Environ Monit Assess 188(4):233–256

APHA (2005) Standard methods for examination of water and wastewater, 21st edn. American Public Health Association, Washington, DC

Bruni J, Canepa M, Cipolli F, Chiodini G, Cioni R, Cipolli F, Longinelli A, Marini L, Ottonello G, Zuccolini MV (2002) Irreversible water-rockmass transfer accompanying the generation of the neutral, Mg-HCO3 and high-pH Ca-OH spring waters of the Genova province Italy. Appl Geochem 17(455):474

Dermatas D, Mpouras T, Chrysochoou M, Panagiotakis I, Vatseris C, Linardos N, Theologou E, Boboti N, Xenidis A, Papassiopi N, Sakellariou L (2015) Origin and concentration profile of chromium in a Greek aquifer. J Hazard Mater 281:35–46

DSI (2016) Eastern Mediterranean basin master plan report. General Directorate of State Hydraulic Works of Turkey, Ankara

EFSA Contam Panel (EFSA Panel on Contaminants in the Food Chain) (2014) Scientific opinion on the risks to public health related to the presence of chromium in food and drinking water. EFSA J 12(3):3595

EPA (2019) Chromium in drinking water. https://www.epa.gov/dwstandardsregulations/chromium-drinking-water Accessed 27 Mar 2020

EU Directive 98/83/EC of 3rd November 1998 on the quality of water indented for human consumption. Official Journal of the European Communities, 05/12/1998, L330/32-54

Fantoni D, Brozzo G, Canepa M, Cipolli F, Marini L, Ottonello G, Vetuschi Zuccolini M (2002) Natural hexavalent chromium in groundwaters interacting with ophiolitic rocks. Environ Geol 42:871–882

Guler C, Kurt MA, Alpaslan M, Akbulut C (2012) Assessment of the impact of anthropogenic activities on the groundwater hydrology and chemistry in Tarsus coastal plain (Mersin, SE Turkey) using fuzzy clustering, multivariate statistics and GIS techniques. J Hydrol 414–415:435–451

Guler C, Kaplan V, Akbulut C (2013) Spatial distribution patterns and temporal trends of heavy-metal concentrations in a petroleum hydrocarbon-contaminated site: Karaduvar coastal aquifer (Mersin, SE Turkey). Environ Earth Sci 70:943–962

Hatipoglu Z (2004) Hydrogeochemistry of Mersin-Tarsus coastal aquifer (in Turkish with English abstract). PhD Thesis, Hacettepe University, Institute of Pure and Applied Sciences, Turkey, 142 pp

Hatipoglu Z, Motz L, Bayari CS (2009) Characterization of the groundwater flow system in the hillside and coastal aquifers of the Mersin-Tarsus region (Turkey). Hydrogeol J 17(7):1761–1778

Margiotta S, Mongelli G, Summa V, Paternoster M, Fiore S (2012) Trace element distribution and Cr(VI) speciation in Ca-HCO$_3$ and Mg-HCO$_3$ spring waters from the northern sector of the Pollino massif, southern Italy. J Geochem Explor 115:1–12

Mitrakas M, Tzoupanos ND, Kazakis N, Kaprara E, Simeonidis K, Samaras P, Zouboulis AI (2012) Hexavalent chromium [Cr(VI)] in drinking water of Greece-Estimation of the origin. In: CRETE 2012, 3rd international conference on industrial and hazardous waste management, 12–14 Sept 2012, Chania, Crete, Greece

Oze C, Fendorf S, Bird DK, Robert G (2004) Chromium geochemistry of serpentine soils. Int Geol Rev 46:97–126

Oze C, Bird DK, Fendorf S (2007) Genesis of hexavalent chromium from natural causes in soil and groundwater. PNAS 104:6544–6549

Panagiotakis I, Dermatas D, Vatseris C, Chrysochoou M, Papassiopi N, Xenidis A, Vaxevanidou K (2015) Forensic investigation of a chromium(VI) groundwater plume in Thiva Greece Vaxevanidou. J Hazard Mater 281:27–34

Parlak O (1996) Geochemistry and geochronology of the Mersin ophiolite within the Eastern Mediterranean Tectonic Frame. PhD thesis, Terre & Environment 6, University of Geneva, Switzerland

Senol M, Sahin S, Duman TY (1998) The geological investigation of Mersin region. General Directorate of Mineral Research and Exploration of Turkey, Ankara (in Turkish)

Silva B, Figueiredo H, Quintelas C, Neves IC, Tavares T (2008) Zeolites as supports for the biorecovery of hexavalent and trivalent chromium. Microporous Mesoporous Mater 116(1–3):555–560

Van Camp M, Walraevens K (2008) Identifying and interpreting baseline trends. In: Edmunds WM, Shand P (eds) Natural groundwater quality. Blackwell, Boston, MA, pp 131–154